

## EFFECT OF Nb ON LAMELLAR ORIENTATION CONTROL OF SINGLE CRYSTAL GAMMA TiAl ALLOYS WITH FULLY LAMELLAR MICROSTRUCTURE

Masao Takeyama<sup>1</sup>, Yukinori Yamamoto<sup>1</sup>, Masato Nagaki<sup>1</sup>,  
Kiyoshi Hashimoto<sup>2</sup>, Takashi Matsuo<sup>1</sup>

<sup>1</sup> Department of Metallurgy and Ceramics Science, Tokyo Institute of Technology  
2-12-1 Ookayama, Meguro-ku, Tokyo 152-8552, JAPAN

<sup>2</sup> Materials Design Technology Co., Ltd., 2-5 Odenma-cho, Nihonbashi, Chuo-ku,  
Tokyo 103-0011, JAPAN

Keywords: Lamellar orientation control, Unidirectional solidification, EBSD analysis, Lattice stability, Liquidus surface of Ti-Al-Nb system, Thermal stability of lamellar microstructure

### Abstract

Lamellar orientation control of Ti-48Al-8Nb unidirectionally solidified using a seed of  $\gamma$  single phase Ti-57Al single crystal has been examined by electron backscatter diffraction (EBSD), and the results are compared with those of binary Ti-48Al grown crystal. Both alloys become single crystal with fully lamellar microstructure (PST), although several lamellar grains are formed above the seed crystal. While the binary PST crystal does not always follow the seed orientation, the ternary grown crystals always follow the seed orientation with  $\langle 1\bar{1}0 \rangle_{\gamma}$  direction parallel to that of the seed. Addition of Nb improves the fitness of the lattice parameters between the grown and seed crystals, and also suppresses the peritectic reaction ( $L+\alpha \rightarrow \gamma$ ). The liquidus projection in Ti-Al-Nb ternary system is calculated based on lattice stability of  $\beta$ -Ti,  $\alpha$ -Ti,  $\gamma$ -TiAl and liquid phases, and it is found that the alloys with compositions to be  $\alpha$  solidification in average by mixture of the seed composition could follow the seed orientation. Addition of Nb drastically decreases the fraction of energetically unstable variant interfaces, thereby stabilizing the lamellar microstructure at elevated temperatures.

### Introduction

Gamma-TiAl based alloys with high amounts of niobium have been developed for high temperature structural applications because niobium addition improves both oxidation resistance and strength at elevated temperatures [1-3]. One of the cast alloys containing Nb has already been practically in use for automobile turbocharger blade [3], so the element seems to be indispensable for the gamma alloys to be used at elevated temperatures. For the past several years, we have examined the effect of Nb on the microstructure control of  $\gamma$  alloys [4-7]. Our phase diagram study on Ti-Al-Nb ternary system revealed that a large amount of niobium can be dissolved in both  $\alpha$  and  $\gamma$  phases almost equally, i.e. 9 at.% at 1473 K, and the three-phase coexisting region of  $\beta+\alpha+\gamma$  moves toward high niobium concentration along the equi-aluminum concentration line as temperature increases from 1273 K to 1713 K. Based on this study, it is found that there exists a wide composition range where the  $\alpha$  single-phase region at higher temperatures and  $\gamma$  single-phase region at lower temperatures, with the two-phase region between them [6]. By using the  $\alpha$  to  $\gamma$  phase transformation pathway in Ti-48Al-8Nb (at.%), we

successfully made a fully lamellar single crystal (PST) consisting of almost  $\gamma/\gamma$  interfaces by unidirectional solidification [8]. We also revealed that niobium addition makes the lamellar formation kinetics sluggish, leading to the occurrence of  $\alpha \rightarrow \gamma$  massive transformation even under relatively slow cooling conditions [6]. Another emphasizing point to be noticed is that niobium is partitioned to  $\alpha$  and  $\gamma$  phases equally [4-7], indicating no segregation of Nb at the lamellar interfaces formed along the  $\alpha \rightarrow \gamma$  transformation pathway. All of these features on Nb for gamma alloys are very attractive and actually effective in controlling the microstructure suitable for high temperature applications.

There are two ways to go for R&D on gamma alloys; one is wrought alloy development to be used below 1073 K and the other is cast alloy development targeted above 1073 K. We have recently developed the promising wrought gamma alloys and successfully hot-forged them by using high-temperature bcc  $\beta$ -Ti phase effectively [9-11]. However, most of the alloy development activities in the past decade have been focused on the temperature range above 1073 K in order to replace nickel-base superalloys. In this temperature range, creep strength is important, and alloys with fully lamellar structure are found to show better creep strength than those with duplex structure as well as near gamma structure [12]. In order to further improve the creep strength, single crystallization by unidirectional solidification (UDS) is effective, just like nickel base superalloys. However, due to the  $\alpha \rightarrow \gamma$  phase transformation during cooling, the resulting microstructure becomes PST with fully lamellar structure with no grain boundaries [13, 14], and the creep strength depends strongly on the lamellar orientation with respect to the loading axis [15-18]. Matsuo et al. revealed that the creep resistance of Ti-48Al PST crystal with the lamellar plates aligned parallel to the loading axis is higher by three order of magnitude than that inclined  $45^\circ$  against the loading axis, and also superior to that of the fully lamellar polycrystalline alloy [15-18]. Thus, controlling the lamellar orientation of PST is very important from the engineering viewpoint. However, no one has ever successfully established the method to control the lamellar orientation of PST crystal. Takeyama et al. [19-22] has systematically investigated the lamellar orientation control of Ti-48Al PST crystal, and revealed that using a  $\gamma$  single phase seed of Ti-57Al single crystal is promising to control the lamellar orientation of grown PST crystal [19, 20]. They attributed the mechanism to follow the seed orientation to both the formation of primary  $\alpha$  phase on the top of the seed and the composition travel to skip the peritectic reaction of  $\gamma \rightarrow L + \alpha$ . These results suggest a possibility to control the lamellar orientation of multi-component PST crystal if the reliable phase diagram near melting temperature of the system is established.

From the above viewpoints, thus, Ti-48Al with a high amount of Nb has been unidirectionally solidified by floating zone method using a seed of the  $\gamma$  single phase Ti-57Al single crystal, and the effect of Nb on the lamellar orientation control of the PST crystal has been examined in terms of the both crystallographic as well as phase diagram considerations. In addition, the thermal stability of the lamellar microstructure in the PST crystals with and without niobium has been evaluated.

### Experimental Procedures

Alloys used in this study are Ti-48Al-8Nb (at.%) and Ti-48Al as master ingots and Ti-57Al single crystal as a seed. Master ingots were prepared by induction skull melting, followed by centrifugal casting to a bar shape with 14 mm in diameter and 150 mm in length. Chemical analysis of the ingots revealed the composition of Ti-48.1Al-8.1Nb and Ti-47.8Al, respectively, with oxygen level of 500 ppm by weight. The seed alloy was prepared by arc melting in argon, followed by drop casting to a bar shape with 8 mm in diameter and 80 mm in length. The single crystal seed was produced by UDS using an optical floating zone (OFZ) furnace under a

flowing argon at a growth rate of 20 mm/h. The growth orientation was analyzed by X-ray back-reflection Laue method, and it is oriented about  $10^\circ$  away from  $\langle 100 \rangle_\gamma$ . The Ti-48Al alloys with and without Nb were unidirectionally solidified by OFZ method using the seed crystal under flowing argon. The tip of the master ingot and the seed crystal attached to upper and lower rods of the furnace, respectively, were first partially melted, then put them together and held for 10s, followed by growing at a growth rate of 5 mm/h under flowing argon. In order to examine the primary solidification phase during crystal growth, the UDS process was interrupted by shut off the lamp power source of the furnace. Note that all of the grown crystals eventually become PST crystals although several grains were formed above the seed crystal.

The obtained grown PST crystals with the seed were cut vertically perpendicular to the lamellar plates. A piece of the samples cut from PST crystals was aged at 1473 K for various periods of time up to 9.1 Ms in order to evaluate the niobium effect on the thermal stability of lamellar structure. Microstructures of these samples were examined by optical and scanning electron microscopes. The samples were mechanically and electrochemically polished in a solution of ethanol with 6 vol.% perchloric acid at 233K, followed by etching in a distilled water with 0.75 vol.% HF and 1.7 vol.% HCl. TEM discs were also prepared from the aged samples by twin-jet polishing in the same chemical solution at 253 K. Crystallographic orientation analysis of the grown and seed crystals was performed by electron backscatter diffraction pattern (EBSD) technique, by taking into consideration of the tetragonality ( $c/a=1.02$ ) of  $L1_0$  structure.

## Results & Discussion

### Effect of Nb on Lamellar Orientation Control

#### A. Orientation relationship between grown and seed crystals

The PST crystals of both alloys with and without Nb can be obtained with no difficulties, by reducing the diameter intentionally to about 3 mm at the initial stage of crystal growth. Figure 1 shows a whole outlook of the grown Ti-48Al-8Nb crystal by UDS. The size of grown crystal is about 11 mm in diameter and 150 mm in length. Figure 2 shows a close view near the contact interface between the grown and seed crystals, together with the microstructure of its vertical section. There are several lamellar grains formed just above the interface, but the right-hand grain in Fig. 2 (b) is selectively grown to become PST crystal, as is seen in Fig. 2 (a). Note that the contact interface is fairly flat and no grains are observed within the seed, maintaining the single crystal, consistent with the binary alloys reported previously [19, 20].

All of the lamellar grains formed above the seed crystal in the Nb containing alloy always follow the seed orientation, whereas some of them in the binary alloy do not. Figure 3 shows (111) pole figures of the seed crystal (b) and the lamellar grains (c, d, e), together with the schematic view of the grown Ti-48Al-8Nb crystal (a). Note that the grain marked (c) is

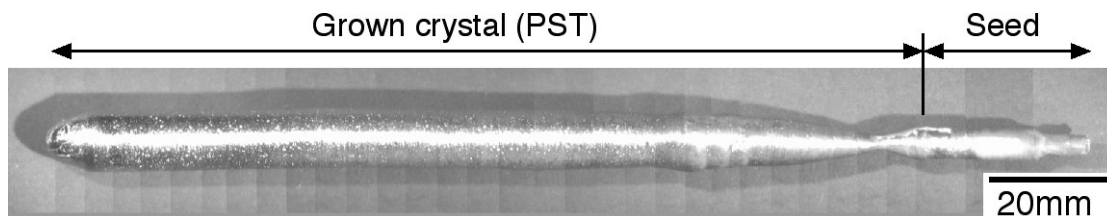


Figure 1. An outlook of the grown Ti-48Al-8Nb crystal by unidirectional solidification using a seed of Ti-57Al single crystal.

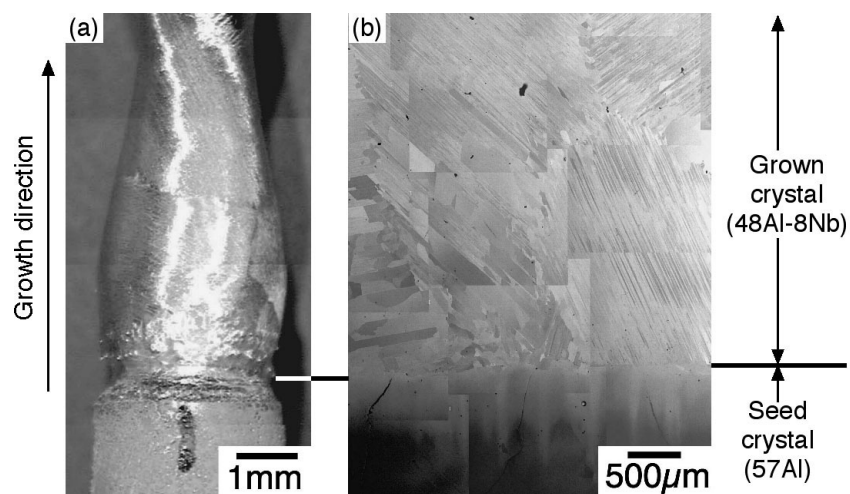


Figure 2. A close view of the contact interface between the seed and grown Ti-48Al-8Nb crystal (a), and the corresponding BEI of the vertical section near the contact interface (b).

selectively grown to become PST crystal. The normal direction (ND) of each pole figure is parallel to the growth direction. Small open circles in the seed crystal represent the  $\langle 1\bar{1}0 \rangle_{\gamma}$  directions, which can easily be confirmed by (110) pole figure. The large open circle in Figs. 3(c, d, e) represents the  $\{111\}$  plane parallel to the lamellar plates, and its zone circle is also drawn. The lamellar orientation of the grains (c) is completely parallel to one of  $\{111\}$  of the seed, and the grain (d) is rotated to some extent. However, the important fact is that for both grains the  $\langle 1\bar{1}0 \rangle_{\gamma}$  direction on the zone marked by double circles is completely consistent with each other and parallel to that of the seed crystal. The pole figure of the grain (e) does not look like that of the seed, however, it shows a twin relation with the seed, having another set of (111) poles with a twin plane of the large open circle in Fig. 3(c). Note that the  $\langle 1\bar{1}0 \rangle_{\gamma}$  direction is also aligned parallel to that of the seed.

In case of Ti-48Al grown crystal, on the other hand, there exist two lamellar grains formed above the seed as shown in Figure 4 (a), and the right-hand grain marked (c) is selectively grown to become PST crystal. The grain (c) follows the seed orientation because the corresponding (111) pole figure is almost consistent with that of the seed (Figs.4 (b) and (c)). Note that in case of Ti-48Al, it can not be easy to distinguish  $\langle 1\bar{1}0 \rangle_{\gamma}$  and  $\langle 10\bar{1} \rangle_{\gamma}$  directions, but one of them, possibly  $\langle 1\bar{1}0 \rangle_{\gamma}$ , becomes parallel to  $\langle 1\bar{1}0 \rangle_{\gamma}$ . However, as shown in Fig. 4(d), the location of the poles of the grain (d) is quite different from that of the seed even considering the possible twin relations.

The present results clearly demonstrated that in Nb containing alloy whenever the lamellar grains follow the seed orientation, the close-packed direction of  $\langle 1\bar{1}0 \rangle_{\gamma}$  is parallel each other even though the  $\{111\}$  planes are misoriented to some extent, and niobium addition is effective in following the seed orientation. As far as the binary  $\gamma$  single phase alloys are concerned, the lattice parameter  $a$  tends to decrease slightly whereas that of  $c$  increases slightly with increasing aluminum content from 50 to 57 at.% [23-25]. Assuming that all Nb atoms occupy the *Ti*-sublattice sites, the calculated lattice parameters of  $a$  and  $c$  in Ti-50Al changes the same ways with increasing Nb content, and niobium addition reduces the misfit of the lattice parameters along  $a$  and  $c$  axes between the grown and the seed crystals. From this crystallographic

viewpoint, therefore, the reduction of mismatch makes it easier for grown crystal to follow the seed orientation in the Nb containing alloys.

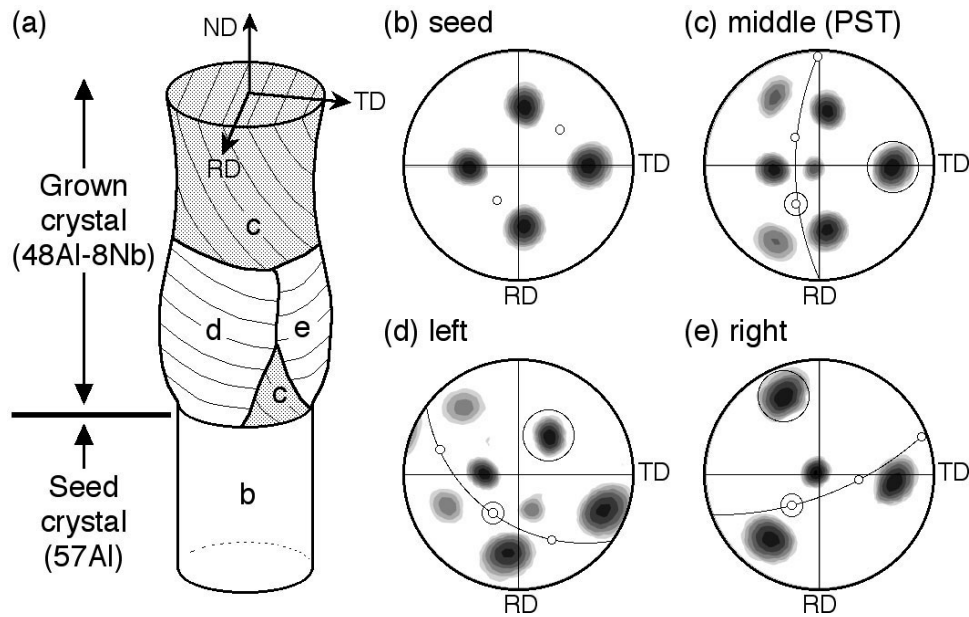


Figure 3. Schematic illustration of Ti-48Al-8Nb grown crystal using the 57Al seed (a), and (111) pole figures of the seed crystal (b) and the lamellar grains above the contact interface (c, d, e): the middle grain (c) is selectively grown to become PST crystal.

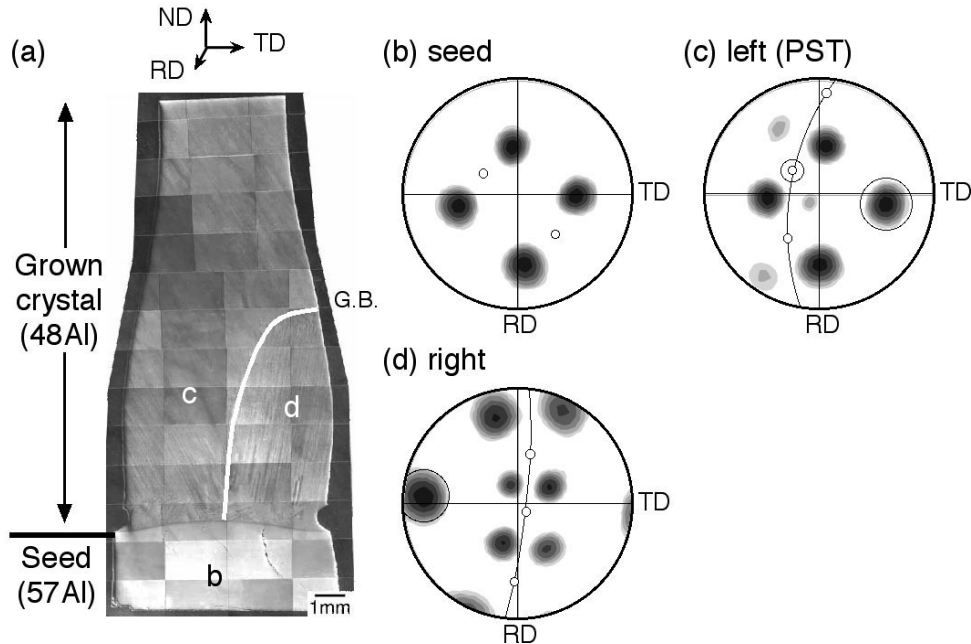


Figure 4. A macroscopic view of the vertical section of Ti-48Al grown crystal with the 57Al seed (a), and (111) pole figures of the seed crystal (b) and the lamellar grains above the contact interface (c, d): the left grain (c) is selectively grown to become PST crystal.

Another point to be considered is the kinetic effect of Nb to suppress the peritectic reaction ( $\gamma \rightarrow L + \alpha$ ). Yamamoto et al. [22] have recently revealed that the longer the holding time of the molten state prior to the crystal growth of Ti-48Al, the more the randomly oriented grain formation above the Ti-57Al seed crystal. They attributed the increase in the number of grains to the progress of peritectic reaction during holding, resulting in the nucleation of random grains at the interfaces. As mentioned earlier, the addition of Nb makes the  $\alpha \rightarrow \gamma$  transformation kinetics sluggish [6], so that it would also slow down the progress of the peritectic reaction, giving less chance to nucleate the grains than the alloy without Nb during the same holding time. Thus, the slow kinetics could also be responsible for the formation of lamellar grains that follow the seed orientation.

### B. Phase diagram considerations

The mechanism to follow the seed orientation requires the formation of primary solidification of  $\alpha$ -Ti phase on the top of the seed crystal. Takeyama et al. [19] revealed that the mixture of  $\beta$  solidification alloy of Ti-48Al and  $\gamma$  solidification seed of Ti-57Al changes its primary phase to  $\alpha$  in its molten state prior to the crystal growth and that the  $\alpha$  phase which follows the seed orientation, transforms to  $\gamma$  phase with Blackburn's orientation relationship during crystal growth, thereby resulting in lamellar structure. In order to extend this to the ternary alloy, the liquidus surface showing primary  $\alpha$  phase region in Ti-Al-Nb ternary system is needed. According to the reports by Perepezko [26] and Kattner [27], the Ti-48Al-8Nb is in  $\alpha$  solidification region as shown in Figure 5, although the trace of the liquid phase compositions in the three-phase coexisting regions of  $L + \alpha + \beta$  and  $L + \gamma + \alpha$  are quite different each other. Based on those studies, the average composition of the grown and seed crystals appears to be in the  $\alpha$

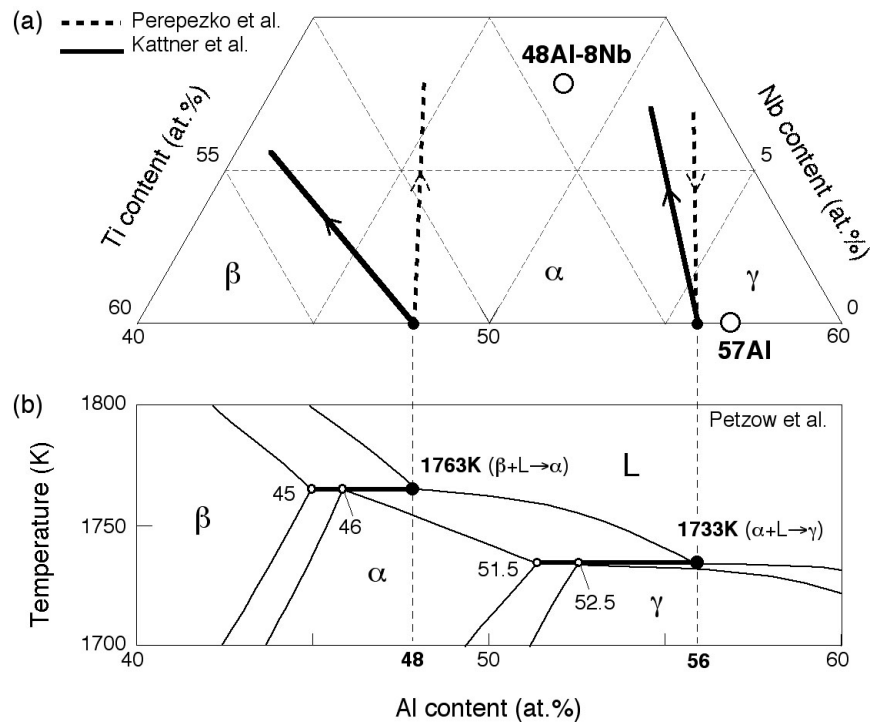


Figure 5. Reported liquidus projection [26, 27] of Ti-Al-Nb ternary system near the two peritectic compositions (a), and Ti-Al binary phase diagram near the melting point (b).

solidification region, so that the mechanism for Ti-48Al-8Nb to follow the seed orientation is likely to be the same as that for the binary 48Al/57Al case. Figure 6 shows an outlook of Ti-48Al-8Nb frozen by rapid cooling during the crystal growth (a) and a BEI of its vertical section near the solid/liquid interface (b). The solidification front exhibits cellular dendritic morphology and the dendrite arms are perpendicular to the dendrite stalks. The fact, together with the composition analysis, revealed that the primary solidification phase of the alloy is not  $\alpha$  but obviously  $\beta$ , inconsistent with those reported diagrams. Thus, it is necessary to establish the reliable liquidus projection of the ternary system.

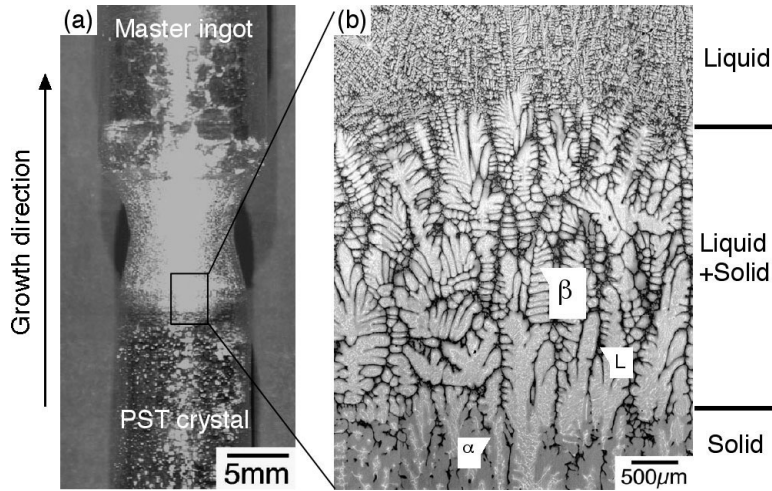


Figure 6. An outlook of the solidification front of the grown Ti-48Al-8Nb PST crystal rapidly cooled during growing (a), and the corresponding BEI of the vertical section near the solid/liquid interface (b).

An attempt has been made to predict the phase equilibria among the phases including liquid phase in Ti-Al-Nb ternary system. Takeyama et al. [6, 7] have reported that the phase equilibria among  $\beta$ ,  $\alpha$  and  $\gamma$  phases in Ti-Al-M ternary systems at elevated temperatures can be interpreted by the ratio of the lattice stability of the M to that of the pure Ti ( $\Lambda_{M/Ti} = \Delta G_M / \Delta G_{Ti}$ ), where the lattice stability is the difference in Gibbs energy of  $\alpha$  phase with different crystal structures, i.e. bcc( $\beta$ ), hcp( $\alpha$ ), fcc( $\gamma$ ), at a given temperature, that is, the phase with bcc structure becomes more stable than that with hcp when  $\Delta G^{\beta \rightarrow \alpha} = G^{\alpha} - G^{\beta} > 0$ . In case that  $\Lambda_{M/Ti} = 1$ , the  $\beta + \alpha$  two-phase field in Ti-Al-M ternary system at a given temperature exists along the equi-aluminum concentration line in the ternary isotherms, indicating that the M has no effect on the relative phase stability between the phases. The larger the value of  $\Lambda$  becomes positive, the more the boundaries of the two-phase field leans toward Al-rich direction, meaning that the addition of M makes the phase stability of  $\alpha$  phase increased relative to  $\beta$ . Then, by extending this lattice stability concept to liquid phase (L), the relative phase stability change among the four phases has been examined.

Figure 7 show the calculated  $\Lambda_{Nb/Ti}$  by using SGTE (Scientific Group Thermodata Europe) between the two of four phases at various temperatures. At temperatures around the two peritectic reactions in the binary system, all of the values between  $\beta/L$ ,  $\alpha/L$  and  $\beta/\alpha$  become 10 or more, and specifically the value of  $\alpha/L$  increases sharply with decreasing temperature. These results suggest that each two-phase field extends toward higher aluminum concentration side as the content of soluble Nb increases, and the Nb effect is more obvious for the  $\alpha + L$  two-phase field. In contrast, the values between  $\alpha/\gamma$  and  $\gamma/L$  are around 1, regardless of temperatures, indicating no Nb effect on the relative phase stability between the two phases. Based on this knowledge, together with the previous results on the movement of the  $\beta + \alpha + \gamma$  three-phase tie-

triangle with temperature [5, 6, 11], a projection of the liquidus surface in Ti-Al-Nb is constructed shown in Figure 8. The detailed interpretation of this phase diagram will be described elsewhere [28], but an important point to be emphasized here is that the alloy of Ti-48Al-8Nb is in  $\beta$  solidification field, consistent with the experimental results. In addition,

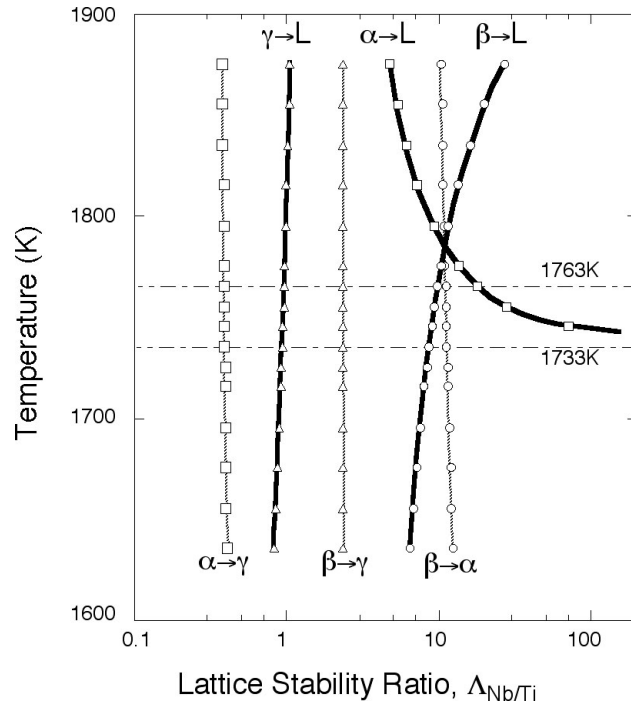


Figure 7. Temperature dependence of lattice stability ratio,  $\Lambda_{\text{Nb/Ti}}$ , among  $\beta$  (bcc),  $\alpha$  (hcp),  $\gamma$  (fcc) and liquid (L) phases.

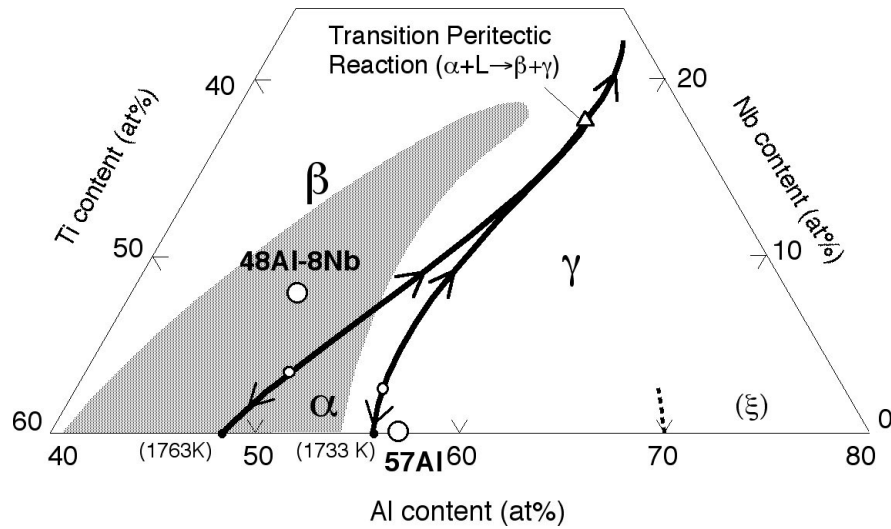


Figure 8. Estimated liquidus projection of Ti-Al-Nb ternary system around two peritectic reactions in Ti-Al binary system, based on the lattice stability ratios.

the average composition between the alloy and the Ti-57Al seed becomes apparently in  $\alpha$  solidification field. This result clearly shows that the mechanism to follow the seed orientation in this ternary alloy is the same as that reported for the binary 48Al/57Al case [19]. The  $\alpha$  solidification field extends toward an equi-aluminum concentration line from the binary edge up to about 15 at.% Nb, so that there is a wide composition range shown by hatching in which the alloys to be grown possibly follow the seed orientation by using a Ti-57Al seed crystal. Although there is still a problem to solve which of the  $\{111\}$  planes in the seed crystal is followed, because of the larger solubility in both  $\alpha$  and  $\gamma$  phases than that of other refractory metals such as Mo and W [5, 7, 29, 30], niobium is the most promising alloying element to make the lamellar orientation control of the ternary PST crystal possible through the adjustment of lattice mismatch against seed crystals.

#### Effect of Nb on thermal stability of lamellar microstructure

Orientation controlled PST crystals are just like a single crystal Ni-base superalloys, so it is very important to understand the thermal stability of the lamellar microstructure at elevated temperatures for their practical applications. The lamellar microstructure formed by  $\alpha \rightarrow \gamma$  transformation consists of  $\gamma$  and  $\alpha(\alpha_2)$  plates, however, because of the tetragonality, there exist three types of  $\gamma/\gamma$  interfaces, together with an  $\alpha/\gamma$  interface: variant interface, perfect-twin and pseudo-twin boundaries. Yamamoto et al. [8, 31-33] already identified the thermal stability of the microstructure of each PST crystal of Ti-48Al and Ti-48Al-8Nb, and revealed that the lamellar microstructure in the binary PST is much more stable than that in the ternary PST crystal when aged at elevated temperatures. However, it does not mean that Nb has a harmful effect on the stability. The instability of the lamellar microstructure in the ternary PST is caused by microstructure effect; the binary lamellar microstructure contains a certain amount of thermodynamically stable  $\alpha_2$  plates, whereas the ternary one has almost no  $\alpha_2$  phase and mostly consists of the  $\gamma/\gamma$  interfaces. Thus, by using the PST in Ti-48Al-8Nb, the role of  $\alpha_2$  plate on the thermal stability of lamellar microstructure, the difference in stability of the  $\gamma/\gamma$  interfaces and the mechanism to collapse the lamellar microstructure can be clearly identified and they were reported elsewhere [8, 31-33].

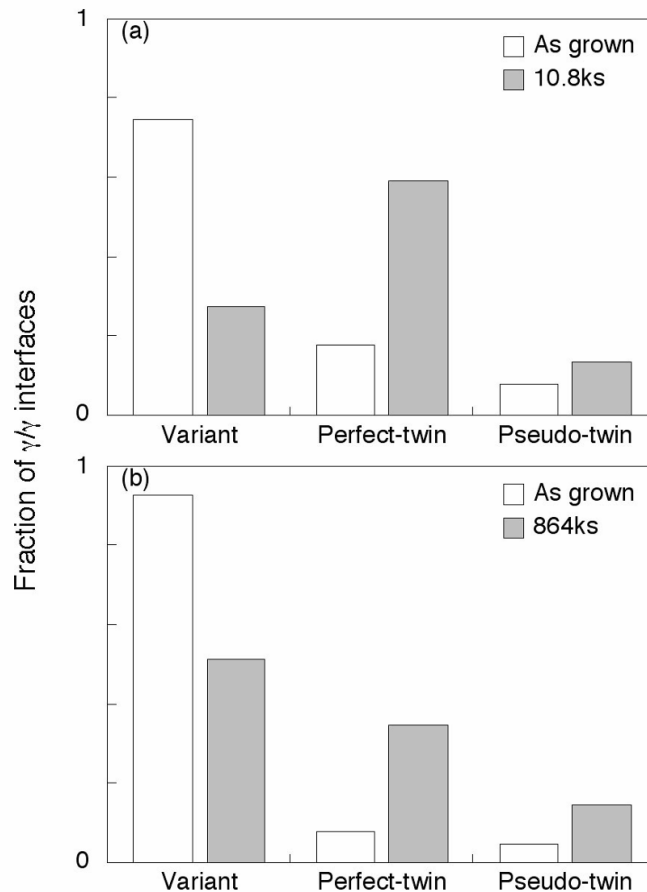


Figure 9. Fraction of the three types of  $\gamma/\gamma$  interfaces within the lamellar microstructure of PST crystals before and after aging at 1473 K: (a) Ti-48Al-8Nb and (b) Ti-48Al.

In order to figure out the pure Nb effect on the stability of the lamellar microstructure in the binary and ternary PSTs, an attention has to be paid only to the  $\gamma/\gamma$  interfaces within the lamellar microstructure. Figure 9 shows the fraction of the types of  $\gamma/\gamma$  interfaces in Ti-48Al-8Nb before and after aging at 1473 K, together with that in the binary Ti-48Al PST. In as grown state, most of the  $\gamma/\gamma$  interfaces are variant interface in both PSTs, regardless of the presence and absence of Nb. However, in the ternary PST aged for 10.8 ks, the perfect twin boundary which is energetically the most stable among the interfaces [32], overwhelmingly becomes major interface, whereas the variant interface is still dominant in the binary PST even after long time aging for 864 ks, although the fraction of the variant interface is reduced and that of the perfect-twin boundary is increased. This result clearly suggests that Nb addition is consequently very effective in stabilizing the lamellar microstructure at elevated temperatures.

Yamamoto et al. [32] revealed that most of the variant interface has curved segments and the extinction of the variant interfaces is caused by interface reaction through the migration of the curved segment. Thus, the rapid change in the type of major interface with aging in the ternary PST is caused by the increase in driving force for the interface migration. As mentioned in the previous section, the addition of Nb decreases and increases the lattice parameters of  $a$  and  $c$ , respectively, and the calculated  $c/a$  ratio increases from 1.016 to 1.032 as Nb content in Ti-50Al increases to 8 at.%. While the interfacial energy of the perfect-twin boundary is basically insensitive to the  $c/a$  ratio, that of the variant interface increases due to the larger atom

mismatch at the interfaces as the ratio increases. Thus, the addition of Nb leads to the large difference in interfacial energy between the two types of interfaces and increases driving force for the interface migration. In addition, the larger the  $c/a$ , the more the interface dislocations at the curved segment of the variant interfaces, thereby leading to the increase in mobility of the interface. These are responsible for the rapid extinction of energetically unstable variant interfaces during the early stage of aging, resulting in the stable lamellar microstructure. Therefore, because of no segregation to the interfaces, addition of Nb to alloys with lower aluminum contents having thermodynamically stable  $\alpha_2$  phase, is expected to maintain the lamellar microstructure stable even after prolonged aging at elevated temperatures.

### Summary

Unidirectional solidification of Ti-48Al alloys adding Nb up to 8at.% has been conducted using a seed of  $\gamma$  single crystal Ti-57Al, and the effect of Nb on the lamellar orientation control of the PST crystals as well as thermal stability of the lamellar microstructure at elevated temperatures have been examined. The following conclusions are drawn in this study:

1. The alloy with Nb becomes single crystal with fully lamellar microstructure (PST) and it consistently follows the seed orientation with a  $\langle 1\bar{1}0 \rangle_\gamma$  direction parallel each other even though the lamellar plane is not parallel to  $\{111\}$  planes of the seed. In contrast, the binary alloy becomes PST with no difficulty but not always follow the seed orientation. The beneficial effect of Nb could be attributed to the following: (1) slower kinetics of a peritectic reaction ( $\gamma \rightarrow L + \alpha$ ) in mixed molten state prior to the growth, (2) better fitting to the lattice parameters between the grown and seed crystals.
2. The alloy with 8%Nb exhibit  $\beta$  solidification whereas the seed shows  $\gamma$  solidification, and the mixture of both alloys becomes  $\alpha$  solidification, which is the key condition to follow the seed orientation. The liquidus projection in Ti-Al-Nb system predicted based on the lattice stability among the four phases of  $\beta$ ,  $\alpha$ ,  $\gamma$  and liquid suggests that there exists a wide composition range up to nearly 15%Nb to follow the seed orientation, and this ternary system is very promising in controlling the lamellar orientation.
3. As grown crystals exhibit an extremely high fraction of energetically unstable variant interface among the three types of  $\gamma/\gamma$  interfaces within the lamellar microstructure, regardless of Nb content. However, the Nb addition drastically reduces the fraction to create energetically the most stable perfect-twin boundaries through the interface reaction by a short time aging at elevated temperatures. This indicates that addition of Nb is effective in improve the stability of the lamellar microstructure.

## Acknowledgements

This research is supported in part by Scientific Research Scholarship (#2-2003) from the foundation "Hattori-hokokai", Japan, and partly by grant-in-aid (14205102) for Scientific Research from Ministry of Education, Culture, Sports, Science and Technology.

## References

1. Z. C. Liu et al., "Effects of Nb and Al on the microstructures and mechanical properties of high Nb containing TiAl base alloys," *Intermetallics*, 10 (2002), 653-659.
2. G. L. Chen et al., "Strengthening mechanism in high Nb containing TiAl base alloys," *Structural Intermetallics 2001*, ed. K. J. Hemker et al., (Warrendale, PA, TMS, 2001), 475-481.
3. T. Tetsui and S. Ono, "Endurance and composition and microstructure effects on endurance of TiAl used in turbochargers," *Intermetallics*, 7 (1999), 689-697.
4. H. Nakamura et al., "Phase Equilibria in TiAl Alloys Containing 10 and 20 at.% Nb at 1473K," *Scripta Metall.*, 28 (1993), 997.
5. H. Nakamura et al., "Phase Equilibria Among The  $\alpha$ ,  $\beta$  and  $\gamma$  Phases in the Ti-Al-X (V, Nb, Cr, Mo) Systems at 1473 and 1573 K," *Intermetallic Compounds for High-Temperature Structural Applications, 3rd Japan Intl. SAMPE Symp.*, ed. M. Yamaguchi and H. Fukutomi (Japan, SAMPE, 1993), 1353-1358.
6. M. Takeyama et al., "Phase Equilibria and Microstructural Control of gamma TiAl based Alloys," *Intermetallics*, 6 (1998), 643-646.
7. M. Takeyama and M. Kikuchi, "Phase Equilibria and Microstructure Evolution of Gamma Titanium Aluminides -Effect of Third Alloying Element on Binary Ti-Al Alloys-," *Materia Japan*, 35 (1996), 1058-1061.
8. Y. Yamamoto et al., "Microstructure Change in Fully Lamellar Ti-48Al-8Nb Single Crystal During Aging at Elevated Temperatures," *Structural Intermetallics 2001*, ed. K. J. Hemker et al. (Warrendale, PA: TMS, 2001), 601-606.
9. T. Tetsui et al., "A newly developed hot worked TiAl alloy for blades and structural components," *Scripta Mater.*, 47 (2002), 399-403.
10. T. Tetsui et al., "Strengthening a high-strength TiAl alloy by hot-forging," *Intermetallics*, 11 (2003), 299-306.
11. S. Kobayashi et al., "Microstructure Control Using  $\beta$ -Titanium Phase for Wrought Gamma TiAl Based Alloys," *Gamma Titanium Aluminides 2003*, ed. Y. W. Kim et al., (Warrendale, PA, TMS, 2003), in print.
12. Y. W. Kim, "Ordered Intermetallic Alloys, Part III: Gamma Titanium Aluminides," *JOM*, 46 (1994), 30-39.
13. T. Fujiwara et al., "Deformation of polysynthetically twinned crystals of TiAl with a nearly stoichiometric composition," *Philosophical Magazine A*, 61 (1990), 591-606.
14. M. Takeyama, T. Hirano and T. Tsujimoto, *Proceeding of International Symposium of Intermetallic Compounds (JIMIS-6)*, ed. O. Izumi (Sendai, Japan: JIM, 1991), 507.
15. T. Matsuo et al., "Effect on Lamellar Plates on Creep Resistance in Near Gamma TiAl Alloy," *Intermetallics*, 6 (1998), 695-698.
16. N. Shiratori et al., "Creep and evolution of dynamic recrystallization in single crystals of Ti-48at%Al with different orientation between stress axis and lamellar plate," *Key Engineering Materials*, 171-174 (2000), 639.

17. T. Matsuo et al., "Role of lamellar plates in creep of TiAl alloy with fully lamellar structure," *Materials Science and Engineering*, A329-331 (2002), 774-779.
18. T. Asai et al., "Microstructure in Ti-48at.%Al PST crystal subjected to creep deformation," *Materials Science and Engineering*, A329-331 (2002), 828-834.
19. M. Takeyama et al., "Lamellar orientation control of Ti-48Al PST crystal by unidirectional solidification," *Materials Science and Engineering*, A329-331 (2002), 7-12.
20. Y. Yamamoto et al., "Control of Lamellar Orientation in  $\gamma$ -TiAl Based PST Crystal by Using Seed Crystals," *High-Temperature Ordered Intermetallic Alloys IX*, ed. J. H. Schneibel et al., 646 (Warrendale, PA: MRS, 2001), N5. 54. 1- N5. 54. 6.
21. Y. Yamamoto et al., "Lamellar Orientation Control of  $\gamma$ -TiAl Based Fully Lamellar Single Crystal," *Report of the 123rd Committee on Heat-Resisting Materials and Alloys*, 41 (Japan Society for the Promotion of Science, 2000), 213-222.
22. Y. Yamamoto et al., "Crystallographic Considerations for Lamellar Orientation Control of Ti-48Al PST Crystal," *Gamma Titanium Aluminides 2003*, ed. Y. W. Kim et al., (Warrendale, PA, TMS, 2003), in print.
23. K. Hashimoto, Doctoral Thesis, Tokyo Institute of Technology (1991).
24. E. S. K. Menon et al., "Accurate determination of the lattice parameters of  $\gamma$ -TiAl alloys," *Journal of Materials Science Letters*, 15 (1996), 1231-1233.
25. H. Erschbaumer et al., "Atomic modelling of Nb, V, Cr, and Mn substitutions in  $\gamma$ -TiAl. I:  $c/a$  ratio and site preference," *Intermetallics*, 1 (1993), 99-106.
26. J. H. Perepezko et al., "High Temperature Phase Stability in the Ti-Al-Nb System," *High Temperature Aluminides and Intermetallics*, ed. S. H. Whang et al. (Warrendale, PA: TMS, 1990), 19.
27. U. R. Kattner and W. J. Boettinger, "Thermodynamic calculation of the ternary Ti-Al-Nb system," *Materials Science and Engineering*, A152 (1992), 9-17.
28. Y. Yamamoto et al., "Lamellar Orientation Control of  $\gamma$ -TiAl Based Fully Lamellar Single Crystal in Ti-Al-Nb Ternary System," *Report of the 123rd Committee on Heat-Resisting Materials and Alloys*, 44 (Japan Society for the Promotion of Science, 2003), 159-165.
29. R. Kainuma et al., "Stability of B2 ordered phase in the Ti-rich portion of Ti-Al-Cr and Ti-Al-Fe ternary systems," *Intermetallics*, 8 (2000), 869-875.
30. S. Kobayashi, Doctoral Thesis, Tokyo Institute of Technology (2002).
31. Y. Yamamoto et al., "Thermal Instability of  $\gamma/\gamma$  Interfaces in Fully Lamellar Ti-48Al Single Crystal Alloys at Elevated Temperatures," *Journal of Materials Processing Technology*, (Warrendale PA: TMS, 2000), CD-ROM, Section E3.
32. Y. Yamamoto et al., "Stability of lamellar microstructure consisting of  $\gamma/\gamma$  interfaces in Ti-48Al-8Nb single crystal at elevated temperatures," *Materials Science and Engineering*, A329-331 (2002), 631-636.
33. Y. Yamamoto et al., "A Mechanism of Polycrystallization in Fully Lamellar Ti-48Al-8Nb Single Crystal Alloy Aged at Elevated Temperatures," *Defect properties and Related Phenomena in Intermetallic Alloys*, ed. E. P. George et al., 753 (Warrendale, PA: MRS, 2002), 255-260.